**Structural Engineering and Mechanics**, *Vol. 72, No. 2 (2019) 155-168*
DOI: https://doi.org/10.12989/sem.2019.72.2.155


# Effectiveness of different confining configurations of FRP jackets for concrete columns

Marina L. Moretti*[1,2]

[1]*Department of Civil Engineering, University of Thessaly, Pedion Areos, Volos 38334, Greece*
[2]*School of Architecture, National Technical University of Athens, Athens 10682, Greece*

*(Received October 21, 2018, Revised May 5, 2019, Accepted May 22, 2019)*

**Abstract.** This paper presents the results of an experimental investigation on the compressive strength of small scale concentrically axially loaded fiber-reinforced polymer (FRP) confined plain concrete columns, with cylinder concrete strength 19 MPa. For columns with circular (150-mm diameter) and square (150-mm side) cross sections wrapped with glass- and carbon- FRP sheets (GFRP and CFRP, respectively) applied with dry lay-up the effect of different jacket schemes and different overlap configurations on the confined characteristics is investigated. Test results indicate that the most cost effective jacket configuration among those tested is for one layer of CFRP, for both types of sections. In square sections the location of the lap length, either in the corner or along the side, does not seem to affect the confined performance. Furthermore, in circular sections, the presence of an extra wrap with FRP fibers parallel to the column's axis enhances the concrete strength proportionally to the axial rigidity of the FRP jacket. The recorded strains and the distributions of lateral confining pressures are discussed. Existing design equations are used to assess the lateral confining stresses and the confined concrete strength making use of the measured hoop strains.

**Keywords:** columns; concrete; cylinders; cubes; fiber reinforced polymer (FRP); overlap; fiber orientation; effectiveness of confinement

## 1. Introduction

External application of fiber reinforced polymer composite (FRP) jackets is a method increasingly more often used for repair and strengthening of reinforced concrete columns in substandard buildings in earthquake-prone regions as many analytical and experimental studies demonstrate (Ilki and Kumbasar 2002, Rousakis and Karabinis 2008, Hou *et al.* 2015, Koçak 2015, Smyrou 2015, Yurdakul and Avsar 2015, Kakaletsis 2016, Tunaboyu and Avşar 2017, Duran *et al.* 2018). It has been established that FRP jackets may considerably increase the mechanical characteristics of concrete subjected to compression because of the lateral confining pressure they exert on the concrete core. The amount of the FRP confinement achieved is maximized in circular cross sections, while it reduces in rectangular sections as the ratio of the long-to-short span increases (Ilki *et al.* 2004, Ozbakkaloglu 2013). The effectiveness of the jacket is often evaluated according to the strain efficiency of the FRP, which is defined as the hoop strain in the FRP jacket at failure to the rupture strain of the fibers or the flat tensile coupons. The strain efficiency has been found to depend, among other factors, on the type of FRP material and cross section, on geometric discontinuities at the ends of the FRP lap length, and on multi-axial state of stress of the FRP jacket (Shahawy *et al.* 2000, Pessiki *et al.* 2001, Harries and Kharel 2002, Lam and Teng 2003, Harries and Carey 2003, Lignola *et al.* 2008, Chen *et al.* 2010, Wu and Jiang 2013, Lim and Ozbakkaloglu 2015).

Though it is well understood that the optimal orientation of the FRP fibers is parallel to the cross section, experimental studies on different combinations of fiber orientations have been realized. Angular FRP jackets are reported to yield more ductile failure modes for axially loaded plain concrete columns (Au and Buyukozturk 2005, Bouchelaghem *et al.* 2011), however, the conclusions regarding the increase in strength are inconsistent. In case of reinforced concrete columns the presence of FRP fibers parallel to the column's axis (longitudinal) are apparently more efficient if another exterior layer of transverse fibers is present (Tan 2002, Issa *et al.* 2009), while Fitzwilliam and Bisby (2010) report that additional longitudinal CFRP wraps reduce lateral deflections of slender columns but have no effect on the respective strength. Moshiri *et al.* (2015) from tests on 500-mm high plain concrete specimens with round (150 mm diameter) and square (133 mm side) cross section report that longitudinal CFRP jackets with different mounting techniques and without the presence of transverse CFRP fibers yield promising results. Sadeghian *et al.* (2010), from testing different combinations of one and two layers longitudinal and transverse FRP fibers on 150/300 mm plain concrete cylinders, conclude that longitudinal fibers do not contribute to the axial strength, irrespective of the stack sequence. In the present study the effectiveness of an additional external jacket with fibers parallel to the column's axis is investigated both for GFRP and CFRP jackets in cylindrical concrete specimens.

*Corresponding author, Assistant Professor
E-mail: moretti@central.ntua.gr

**Copyright © 2019 Techno-Press, Ltd.**
http://www.techno-press.com/journals/sem&subpage=7
ISSN: 1225-4568 (Print), 1598-6217 (Online)

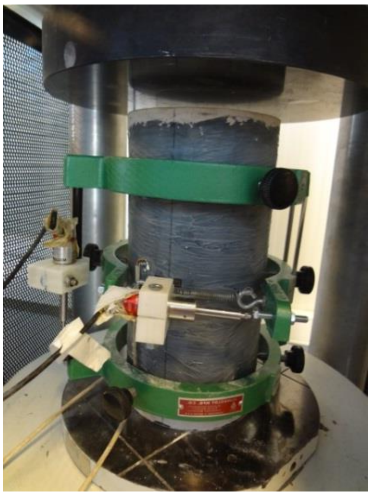

(a) Cylinder (diameter 152 mm, height 305 mm)

(b) Cube (side 150 mm)

Fig. 1 Typical specimens in the compression test machine

FRP jackets in columns with circular cross sections often rupture at the ends of the FRP lap length because of local stress concentrations, according to test results on axially loaded columns (Bisby and Take 2009, Chen *et al.* 2010, Smith *et al.* 2010, Lim and Ozbakkaloglu 2015). For rectangular sections the effect of FRP lap region on the performance of FRP-confined concrete columns has not been investigated, to the best knowledge of the author, while in tests reported in the literature lapping of the FRP jacket is performed either along the side (Roussakis *et al.* 2007) or near one of the corners (Wang *et al.* 2012) of the section, as no specific recommendations are available. In this study the issue of performing the overlap at the corner or along the side is investigated on 4 cubic specimens with 150 mm side.

This paper presents a summary of an experimental investigation on nine axially loaded FRP-confined small-scale specimens with circular and square section, and aims at gaining further understanding of several factors pertaining to the configuration of the FRP lap region and their impact on confinement. The effectiveness of FRP-confined specimens is assessed by the cost efficiency confinement index, which considers also the unit cost of materials used (Bouchelaghem *et al.* 2011, Abdelrahman and El-Hacha 2014), and also by the strain efficiency. Test results are discussed and compared to existing design recommendations (Lam and Teng 2003, Eurocode 2-1-1 CEN 2004, Eurocode 8-3 CEN 2005). The design of the specimens presented benefit of the findings of a complementary study (Moretti and Arvanitopoulos 2018).

## 2. Experimental program

### *2.1 Specimen characteristics*

Nine plain concrete columns with circular and square cross sections, wrapped with carbon- and glass- fiber reinforced polymer jackets, CFRP and GFRP, respectively, were manufactured using dry lay-up process and tested under uniaxial compression (Figs. 1(a)-(b)). The specimens consist of 5 cylinder columns with diameter 152 mm and height 305 mm (152/305 mm), and four cubic specimens with 150 mm side. The jacket configurations tested are depicted in Figs. 2(a) to (i). The FRP fibers were placed so as to be perpendicular to the axis of the specimens, except for two cylinders in which an extra outer layer of the same FRP type was placed with the fibers aligned parallel to the axis of the cylinders, shown in Figs. 2(b)-2(c). In two cylinders with a single layer of CFRP jacket with overlap length $L_f$ = 12 cm, a GFRP strip (Gst) was applied at the end of $L_f$, with strip lengths of 10 cm and 12 cm (Figs. 3(d)-(e)) to improve the anchorage of the CFRP jacket along the lap length. The strip was decided to consist of GFRP, which is capable of deforming so as to better bridge the end of the lap length at the event of debonding.

The values of the jacket overlap lengths were based on the results of a companion study (Moretti and Arvanitopoulos 2018) in which it was found that for 152/305 mm wrapped cylinders with identical jacket characteristics, for GFRP $L_f$ = 1 cm is sufficient to exclude the occurrence of debonding, while for CFRP with $L_f$ = 17 cm some debonding still occurred, for dry lay-up and maturing time equal to 7 days (proposed by manufacturers). All specimens were manufactured and tested in the Structures and Concrete Laboratory of the University of Thessaly. It is noted that one specimen was tested for each configuration, with the restrictions that this imposes on generalizing the findings of this research project.

### *2.2 Specimen identification*

The characteristics of the jackets are reflected on the specimens' labels, as follows: The prefix sq– indicates a square cross section, while no prefix corresponds to a cylindrical specimen. Letters C or G denote one layer of CFRP or GFRP, respectively, and GG two GFRP layers. Jackets with longitudinal fibers are designated by $C\ell$ and $G\ell$, for CFRP and GFRP, respectively. The GFRP strip is designated as Gst followed by the strip length in centimetres (cm). The overlap length, $L_f$, of the jacket is

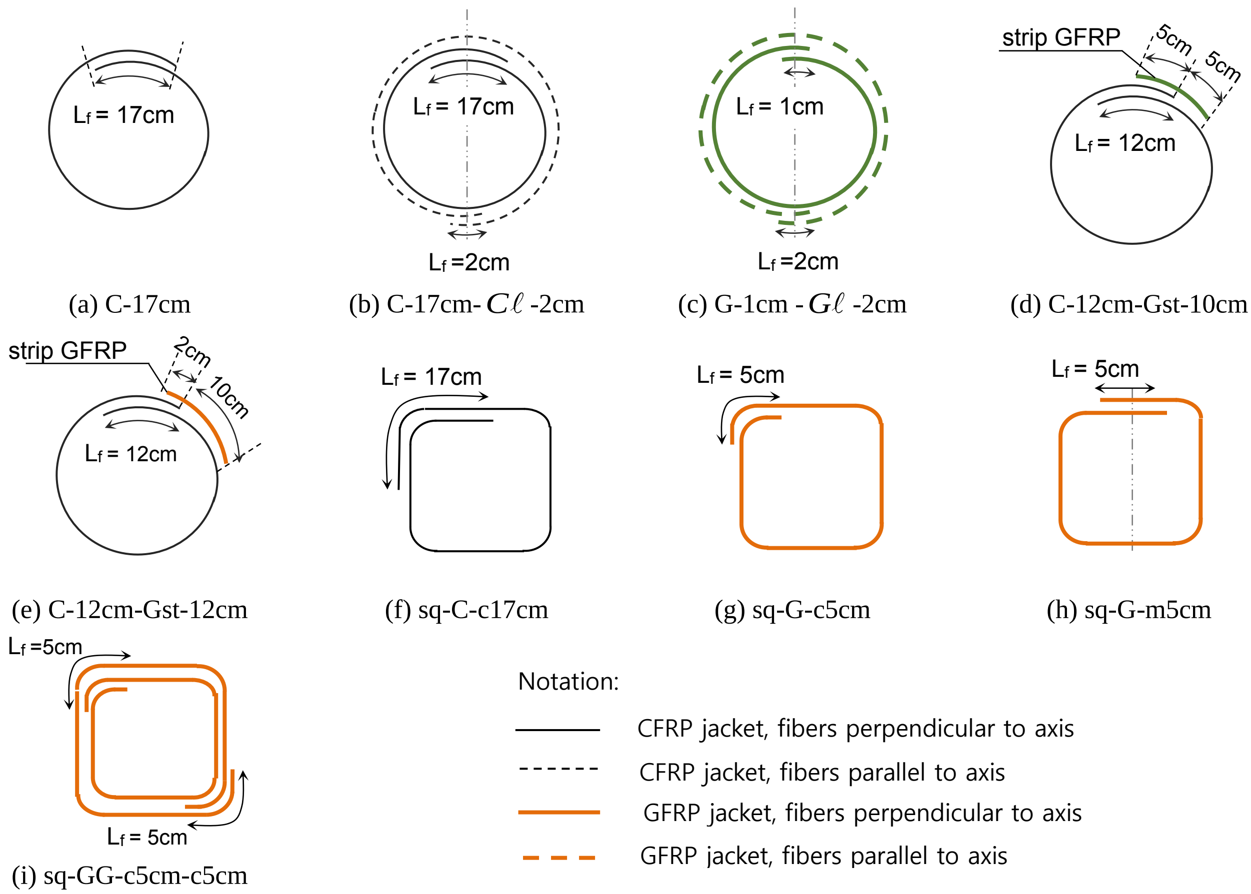


Fig. 2 Configurations of the FRP jackets of the test specimens

given in centimetres (cm) at the end of the label. In square cross sections the lap length is situated symmetrically, either around a corner or in the middle of one side, which is denoted by letters "c" or "m", respectively. In case of two layers the first data correspond to the inner, and the second to the outer FRP jacket. For example, label C-17cm-Cℓ-2cm describes a cylinder specimen, with two CFRP jackets: the inner one with overlap length $L_f$= 17 cm and the outer jacket with fibers at the longitudinal direction and $L_f$ = 2 cm (Fig. 2(b)).

### *2.3 Construction of specimens*

All specimens were cast from the same batch of commercial ready mix concrete. The specimens were removed from the moulds two or three days after casting, and they were cured for 28 days in laboratory conditions. The corners of the square cross sections were rounded at a radius of 25 mm at least 28-days after casting of the cubes, in order to prevent premature rupture of the FRP jacket. It is noted that for rectangular columns and externally bonded FRP jackets, *fib* (2001) proposes rounding of corners with radius of 15 to 25 mm.

Before the application of the FRP jacket the cylinder surface was ground to remove lose particles and other bond inhibiting materials, then cleaned with water and allowed to dry. The dried surface was sprayed with compressed air and then the FRP sheet was applied through dry layup process and left to cure for at least seven days, according to manufacturer's guidelines. The number of days between the FRP application and the test are indicated for each specimen in Table 2 because the factor of curing time of the resin has proved of crucial importance for dry layup process in relation to the occurrence of debonding.

The top and bottom ends of the specimens were strengthened with additional CFRP strips to constrain the location of the FRP rupture in the middle portion of the specimens. These strengthening strips consisted of a single layer of 30-mm and 20-mm height for cylinders and cubes, respectively, and an overlap length equal to 150 mm for all specimens. This practice has been used also in the past at testing FRP confined 152/305 mm cylinders, e.g. single layer of 50 mm wide strips by Lim and Ozbakkaloglu (2015), or multiple layered strips of 25 mm width by Lam and Teng (2004).

### *2.4 Testing and instrumentation*

The specimens were tested under monotonic axial compression using a 3,000-kN capacity universal/ DMG testing machine. Capping material of high compressive strength was applied at both ends of each cylinder to ensure parallel surfaces and uniform distribution of the applied pressure.

Linear variable displacement transducers (LVDTs), mounted on a Humboldt metallic testing frame (Fig. 1(a)),

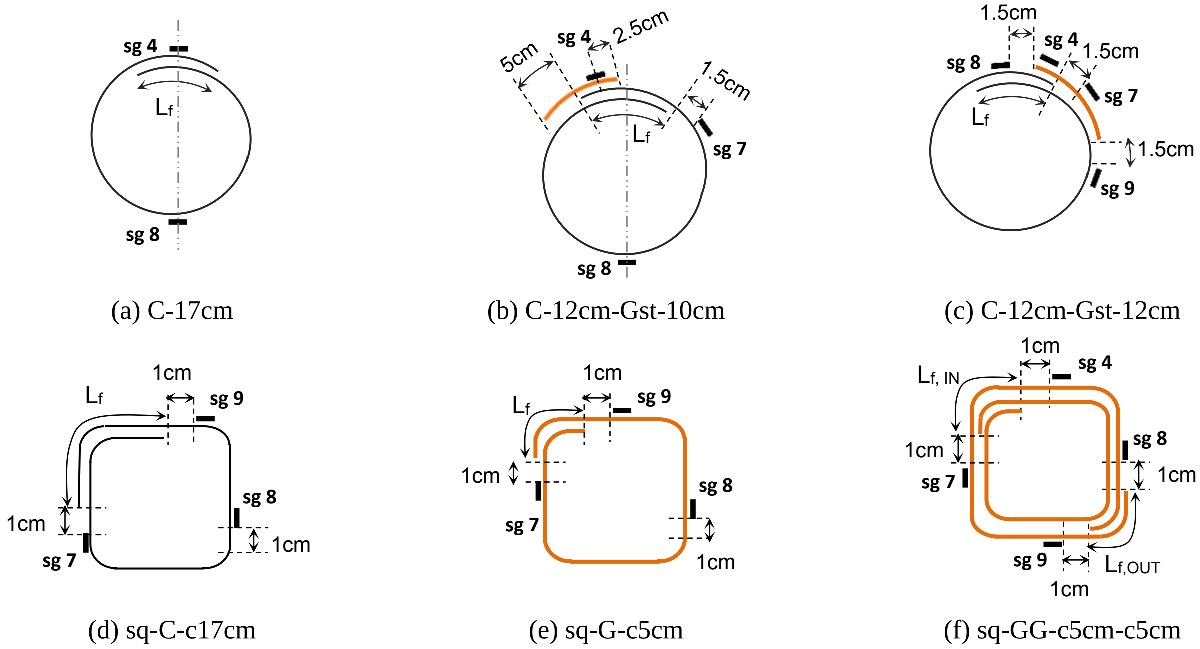


Fig. 3 Location of hoop strain gages at mid-height cross section of the specimens

Table 1 Properties of fiber sheets as provided by the manufacturer

| Type | Nominal thickness $t_f$ (mm/ply) | Tensile strength $f_{fu}$ (MPa) | Ultimate Tensile Strain $\varepsilon_{fu}$ (%) | Elastic Modulus $E_f$ (GPa) | Weight (g/m$^2$) |
|---|---|---|---|---|---|
| Carbon | 0.129 | 4300 | 1.7 | 230 | 235 |
| Glass | 0.172 | 2300 | 2.8 | 76 | 445 |

recorded the average axial (over a length of 203 mm) and lateral strains at mid-height for the 152/305 mm cylinders, $\varepsilon_{cu}$ and $\varepsilon_{lu}$, respectively.

Lateral strains at mid-height of the FRP jackets were measured through two to four unidirectional strain gages placed in the hoop direction, with 20 mm gage length for 152/305 mm cylinders, and with 10 mm gage length for cubes 150 mm. Strain gages were typically placed at the beginning and at the end of the overlap length, at a small distance (equal to 10 and 15 mm for cubes and cylinders, respectively) from the end or start of the overlap length, in order to avoid measuring strain concentrations at the tips of the overlap length (Figs. 3(a) to (f)).

### *2.5 Materials*

The FRP materials used were formed from unidirectional carbon or glass fiber tow sheets (CFRP and GFRP, respectively) and their properties are displayed in Table 1. The same type of a two component epoxy resin was applied onto the concrete substrate as primer, as well as for the FRP application, with tensile modulus 3.5 GPa and rupture strain 1.5%. In all the calculations presented in this work the FRP properties provided by the manufacturers have been assumed.

Ready mix concrete with 28-days cylinder compressive strength equal to 19 MPa was used. All specimens were cast simultaneously but the tests were performed over a four-month period. The unconfined cylinder compressive strength of concrete, $f'_{co}$, was determined from 152/305 mm cylinder and 150 mm cubic test samples (Table 2).

## 3. Test results and discussion

### *3.1 Failure modes*

Figures 4 to 7 show the failure modes recorded. The specimens failed around specimen mid-height by tensile rupture of the FRP jackets. Some FRP debonding occurred only in two cylinders: (a) in specimen C-17cm (7 days curing, see Fig. 4(a)) some debonding along the lap length followed the jacket rupture and (b) in specimen C-12cm-Gst-10cm (8 days curing, see Fig. 5(a)) the GFRP strip debonded from the CFRP substrate. Absence of debonding in C-12cm-Gst-12cm (Fig. 5(b)) can be attributed to the longer GFRP strip and its different location in reference to the lap length of the CFRP jacket, and to the longer FRP curing period of 27 days. Companion specimen C-12cm (not presented in this paper, 8 days curing period) manifested a more extended debonding as may be observed in Fig. 5(c).

The presence of a second FRP layer with the fibers parallel to the specimen axis prevented the occurrence of debonding in CFRP-jacketed specimen C-17cm-Cℓ-2cm and led to a more ductile failure mode with fewer rupture surfaces for both types of FRP as shown in Figs. 6(a)-(b), attributed to fiber reorientation mechanism which results in better energy dissipation (Au and Buyukozturk 2005).


(a) Specimen C-17cm (b) Specimen sq-C-c17cm

Fig. 4 Observed failures for CFRP jacketed cylinder and cube with overlap length $L_f$ = 17 cm


(a) C-12cm-Gst-10cm (b) C-12cm-Gst-12cm (c) C-12cm[(1)]

Fig. 5 Observed failures for CFRP jacketed 152/305 mm cylinders with overlap length $L_f$ = 12 cm, with and without GFRP strip ([(1)] test results reported in Moretti and Arvanitopoulos 2018)

(a) C-17cm-Cℓ-2cm (b) G-1cm-Gℓ-1cm

Fig. 6 Failures of 152/305 mm cylinders with two jackets with fibers in two perpendicular directions

In the cubes vertical FRP rupture occurred either at the end of overlap length, $L_f$, or at the end of a corner in the vicinity of the tip of $L_f$ as illustrated in Fig. 4(b) and Figs. 7(a) to (c). This conforms with previous observations that rectangular FRP-jacketed columns typically fail by FRP rupture at one of the corners (Roussakis *et al.* 2007, Youssef *et al.* 2007, Raval and Dave 2013) because of the discontinuity at the location where the side of the section transitions into the quarter-circular corner (Harries and Carey 2003).

### *3.2 Axial stress - strain behavior*

Table 2 reports the ultimate condition of the specimens, namely: The axial stress recorded just before failure, $f'_{cc}$, the respective maximum hoop strain, $\varepsilon_{h,\max}$, measured from strain gages, as well as the axial and lateral strains, $\varepsilon_{cu}$ and $\varepsilon_{lu}$, recorded by LVDTs.

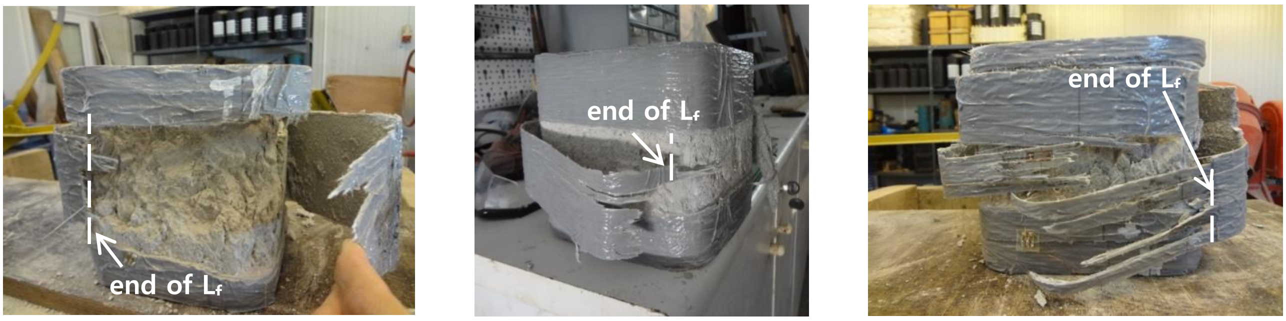


(a) Specimen sq-G-c5cm (b) Specimen sq-G-m5cm (c) Specimen sq-GG-c5cm-c5cm

Fig. 7 Failures for 150 mm cubes with $L_f$ = 5 cm, lapped either along a corner or at the middle of a side

Table 2 Specimen characteristics and test results

| specimen | $f'_{cc}$ (MPa) | $f'_{co}$ (MPa) | Days from FRP application to testing | $\varepsilon_{h,max}$ (‰) | $\varepsilon_{cu}$ (‰) axial | $\varepsilon_{lu}$ (‰) lateral | $f_{lu,aver}$ (MPa) | $\frac{f_{lu,aver}}{f'_{co}}$ | $\frac{\varepsilon_{h,max}}{\varepsilon_{fu}}$ | $E_{eff,conf}$ |
|---|---|---|---|---|---|---|---|---|---|---|
| C-17cm | 36.75 | 19.3 | 7 | 10.49 | 14.34 | 16.07 | 4.51 | 0.23 | 0.617 | 0.414 |
| C-17cm-Cℓ-2cm | 45.29 | 19.7 | 25 | 11.79(1) | 16.70 | 15.08 | 4.60(1) | 0.23(1) | 0.694(1) | 0.282 |
| G-1cm-Gℓ-2cm | 28.87 | 19.7 | 16 | 16.59(1) | 10.51 | 16.14 | 2.54(1) | 0.13(1) | 0.593(1) | 0.204 |
| C-12cm-Gst-10cm | 40.06 | 19.3 | 8 | 14.21 | 17.08 | 15.17 | 5.50 | 0.28 | 0.836 | 0.417 |
| C-12cm-Gst-12cm | 41.02 | 19.7 | 27 | 16.19 | 20.35 | 19.89 | 6.20 | 0.31 | 0.952 | 0.406 |
| sq-C-c17cm | 34.17 | 23(3) | 48 | 16.64 | 3.42(2) | n.a. (4) | 2.01 | 0.09 | 0.979 | 0.348 |
| sq-G-m5cm | 27.03 | 23(3) | 8 | 10.50(5) | 7.01(2) | n.a.(4) | 0.61(5) | 0.03(5) | 0.375(5) | 0.321 |
| sq-G-c5cm | 25.46 | 23(3) | 48 | 17.08 | 2.81(2) | n.a.(4) | 0.92 | 0.04 | 0.610 | 0.302 |
| sq-GG-c5cm-c5cm | 30.04 | 23(3) | 48 | 13.02 | 6.11(2) | n.a.(4) | 1.46 | 0.06 | 0.465 | 0.178 |

(1)calculated through linear interpolation; strain gages on longitudinal fibers failed before maximum load
(2) from strain gages at specimen's mid-height (20 mm gage length)
(3) from 150 mm cubes
(4) not applicable
(5) only one strain gage (the others stopped functioning)

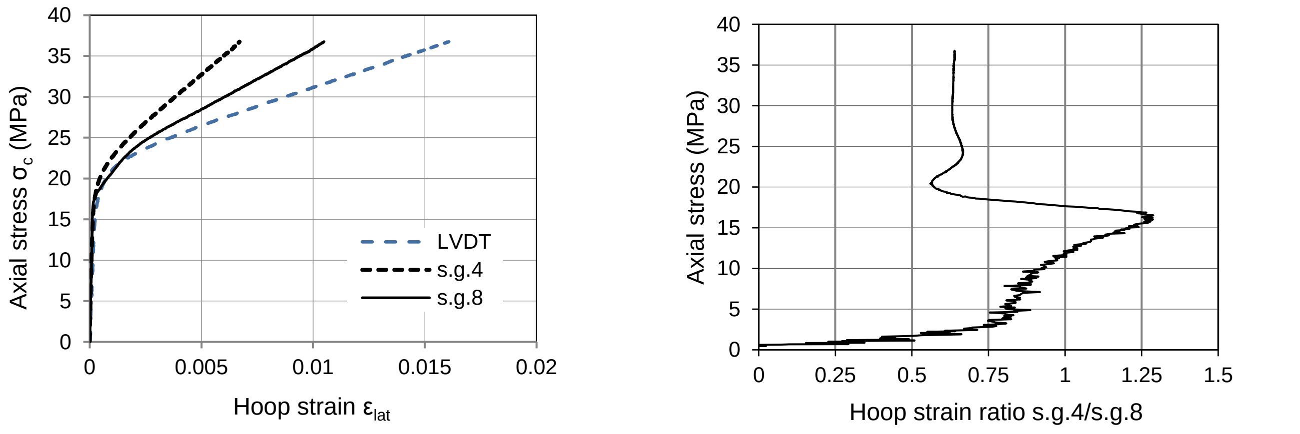


(a) axial stress-lateral strain from LVDT and strain gage (s.g.) measurements (b) axial stress-lateral strain ratio at FRP jacket overlap/non-overlap location

Fig. 8 Axial stress-lateral strain relationships of test specimen C-17cm

### *3.2.1 Specimens wrapped with FRP fibers parallel to cross-section*

Cylindrical specimens

Fig. 8 displays the axial stress-lateral strain relationship for specimen C-17cm as measured from the LVDT and from strain gages situated on the axis of the overlap length (s.g.4) and at a point diametrically opposite to it (s.g.8). Similar stress-strain diagrams are displayed in Figs. 9-10 for specimens C-12cm-Gst-10cm and C-12cm-Gst-12cm, respectively. The exact locations of the 20-mm strain gages are shown in Fig. 3.

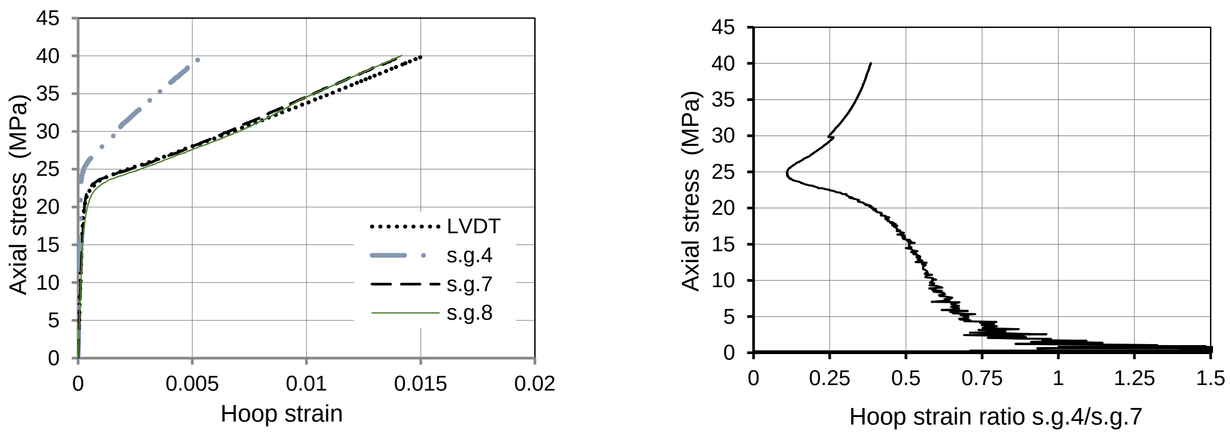


(a) LVDT and strain gage (s.g.) measurements (b) axial stress-lateral strain ratio

Fig. 9 Axial stress-lateral strain relationships for specimen C-12cm-Gst-10cm

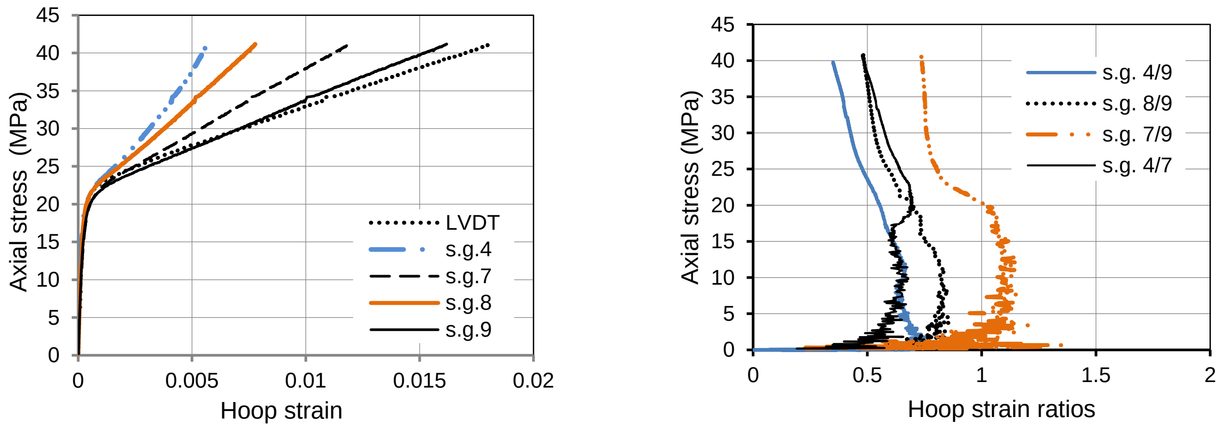


(a) LVDT and strain gage (s.g.) measurements (b) axial stress-lateral strain ratios

Fig. 10 Axial stress-lateral strain relationships for specimen C-12cm-Gst-12cm

In round cross sections the hoop strain ratio from strains measured at different locations of the cross section perimeter tends to stabilize at a specific value at axial stresses higher than the unconfined concrete strength (Fig. 8(b)), while in case of failure attributed to FRP debonding the strain ratio shows an abrupt alteration near ultimate strength (Moretti and Arvanitopoulos 2018).

In specimen C-12cm-Gst-10cm strain ratio s.g.4/s.g.7 increases constantly up to failure (Fig. 9(b)), an evidence of gradual slippage with the increase of axial load, which possibly relates to the observed debonding of the GFRP strip at failure. It is noted that s.g.4 was located close to the end of the GFRP strip and also near the end of overlap length of the underlying CFRP jacket, while s.g.7 was placed on a single CFRP layer (Fig. 3(b)).

Similarly, Figs. 10(a)-(b) show that in specimen C-12cm-Gst-12cm the hoop strains of s.g.4 (located at the tips of GFRP strip and the underlying end of lap length) tend to constantly decrease until failure compared to the hoop strains in other locations. The strain ratio at overlap/non-overlap of the CFRP jacket (s.g.8/s.g.9) stabilizes at 0.47, close to the theoretically expected 0.50. This behavior may indicate a local slippage at the location of s.g. 4 which was successfully absorbed by the GFRP strip given that no debonding was recorded at failure.

The distributions of lateral strains along the cross section at mid-height of specimens C-12cm-Gst-10cm and C-12cm-Gst-12cm for different loading levels are displayed in Figs. 11(a)-(b). Before the activation of the FRP jacket, i.e. for axial stress about (0.85-1) $f'_{co}$, all the strains are almost uniform. After the activation of the jacket smaller strains are measured where more layers of FRP are present, while the lateral confining pressures exerted from the FRP jacket to the concrete core are similar, as validated in section 3.3.

*Cubic specimens*

Fig. 12 depicts hoop strain distributions measured from strain gages along the mid-height section of the cubic specimens for different axial strain values. In general higher strains were measured at the end of the external lap length, which agrees with previous observations from circular FRP wrapped concrete columns (Smith *et al.* 2010, Chen *et al.* 2010 and 2013). The location of the lap length does not appear to have any other influence on the strain distribution of the FRP jackets.

It has been reported that in rectangular FRP-wrapped sections higher values of strains are measured in the middle of the side compared to the corners both for FRP jackets (Harries and Carey 2003) as well as FRP tubes

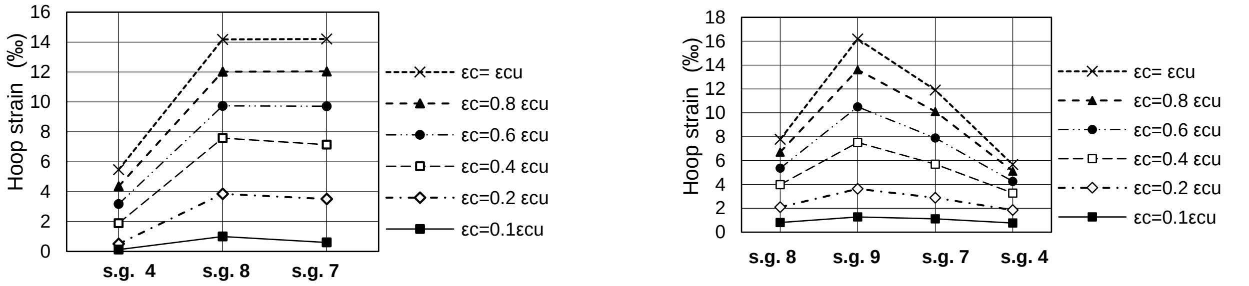


(a) specimen C-12cm-Gst-10cm (b) specimen C-12cm-Gst-12cm

Fig. 11 Distributions of lateral strains along the mid-height cross section for different axial strain values

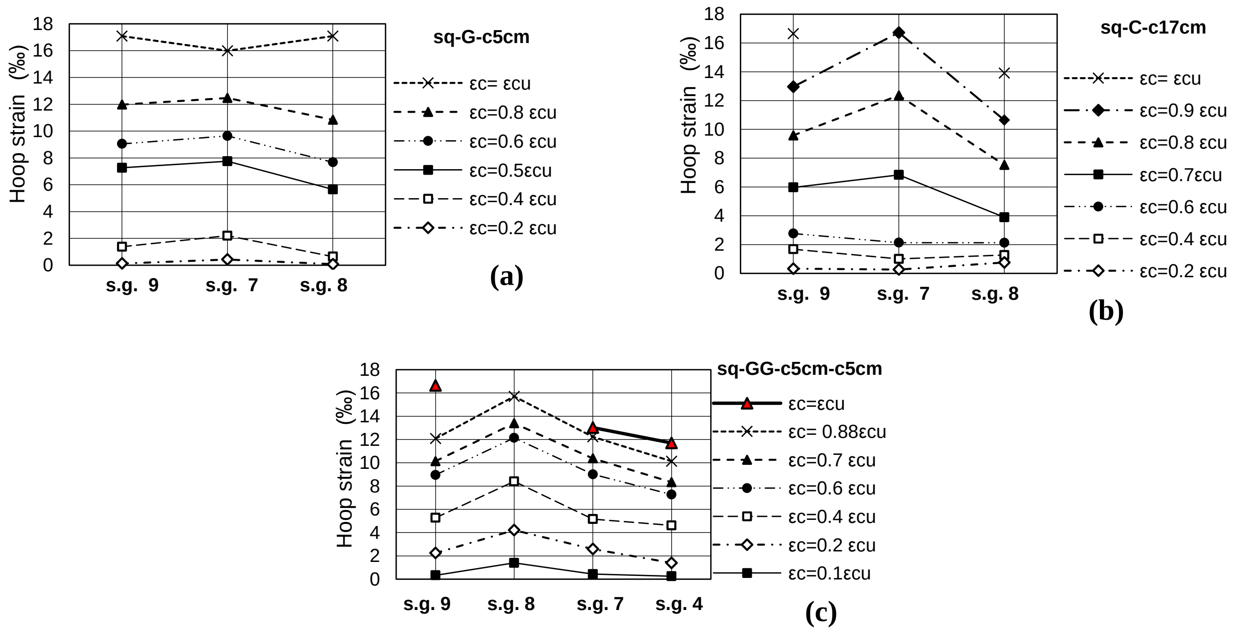


Fig. 12 Distributions of lateral strains along the mid-height cross section of cubic specimen for different axial strain ratios

(Ozbakkaloglu and Oelers 2008, Ozbakkaloglu 2013), because of flexural deformations of the jacket along the sides. To consider this effect Wang *et al.* (2012), from tests on square RC columns (305-mm side) proposed that the effective hoop strain assumed in the FRP jacket at failure should be obtained from averaging only the hoop strains at the corners. In this study strain gages where located only along the side of the cross section, however the lateral pressures calculated from the recorded strains proved to estimate well the confined concrete strength as demonstrated in section 3.4.

### *3.2.2 Effect of FRP fibers in two directions*

The relationships between axial stress-axial and -lateral strain of specimens C-17cm-Cℓ-2cm and C-17cm are shown in Fig. 13. All strains are measured from LVDTs. Contrary to findings of other experimental studies (Sadeghian *et al*. 2010 for 150/300 mm cylinder specimens, with concrete strength 40 MPa), the presence of an additional external CFRP layer with longitudinal fibers leads to a) an increase of axial strain and confined concrete strength of about 20%, and b) a delayed activation of the confining effect of FRP, i.e. the start of the transition zone, of the same percentage. This behavior is attributed to the additional axial (flexural) rigidity of the jacket with longitudinal fibers in specimen C-17cm-Cℓ-2cm. The ascending branches of the two diagrams are parallel, because they are governed by the confining effect of the jacket with the fibers aligned perpendicular to the specimen axis, which is identical for the two specimens. Similar behavior may be observed in Fig. 14 for specimens G-1cm-Gℓ-2cm and G-1cm but with only a 10% increase for G-Gℓ-1cm-2cm because of the lower rigidity of GFRP longitudinal fibers, as discussed also in section 3.4. (Data for G-1cm are available in Moretti and Arvanitopoulos, 2018). It is noted that the observed relatively high increase in the concrete strength because of the presence of a jacket with longitudinal fibers, compared to previous findings in the literature, may be partly attributed to the low concrete strength ($f_{co}$=19 MPa) and to the low aspect ratio of the 150/300 mm specimens.

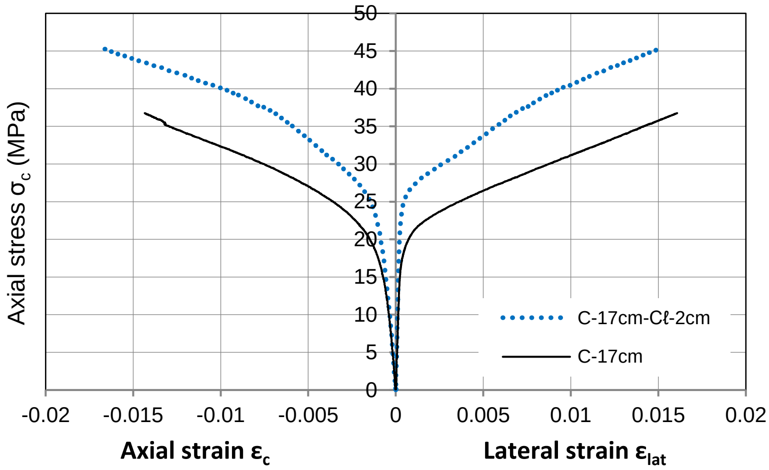


Fig. 13 Axial stress-strain behavior of specimens C-17cm and C-17cm-Cℓ-2cm (curves truncated at peak load)

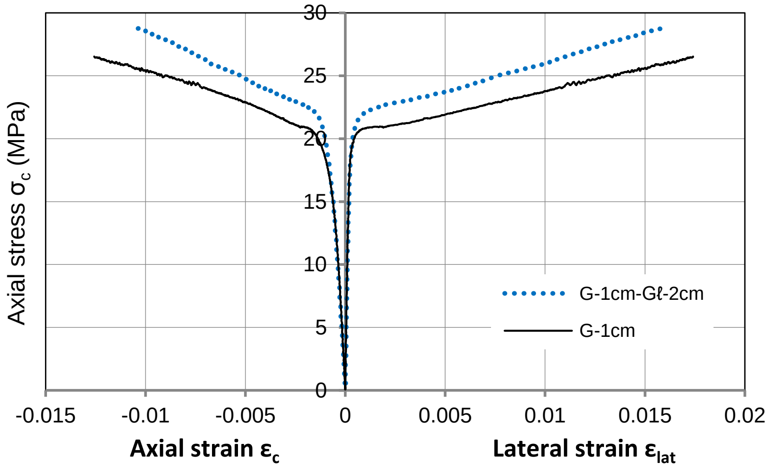


Fig. 14 Comparison of axial stress-strain strain behavior of specimens G-1cm and G-1cm-Gℓ-2cm (curves truncated at peak load)

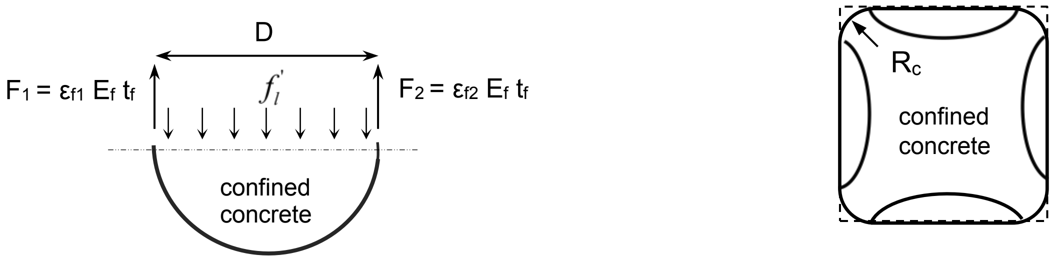


(a) round cross section

(b) square cross section

Fig. 15 Confined concrete core by FFR jacket for different types of cross section

### *3.3 Lateral confining pressure*

In FRP-confined concrete columns subjected to axial compression a lateral confining stress, $f_l'$, is developed in the plane of the cross-section for stresses higher than the unconfined concrete strength after the activation of the FRP jacket. There is general consensus that confinement in circular cross sections provides uniform confining stresses resulting in greater improvement in the member's mechanical characteristics under axial loading, compared to the effect of external confinement in rectilinear sections in which confining stresses are mainly developed across the diagonals of the cross section (Figs. 15(a)-(b)).

#### *3.3.1 Circular cross-section*

For circular cross-sections confining pressure, $f_l'$, is calculated by means of Eq. (1) which assumes that the FRP jacket is uniformly stressed and that the hoop strains, $\varepsilon_{fi}$, at both ends of the cross section diameter at the cut, as well as the respective characteristics of the FRP layers are identical, as displayed on Fig. 15(a). In practice, however, the jacket characteristics are not the same along the section perimeter because of the jacket overlap length. The same is valid also for more complex FRP jacket schemes, e.g. for specimens C-12cm-Gst-10cm and C-12cm-Gst-12cm.

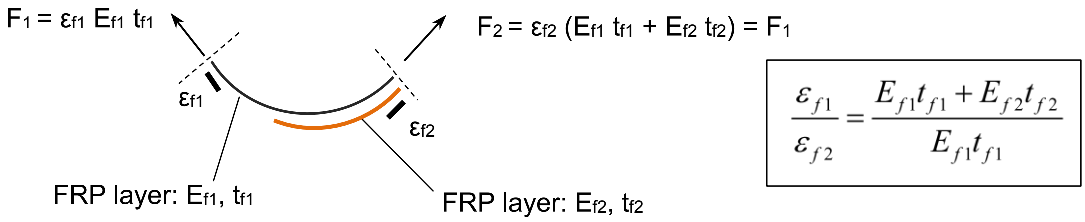


Fig.16 Assumption of constant lateral forces along the perimeter of a jacketed round cross section with different FRP layers and perfect bond between layers

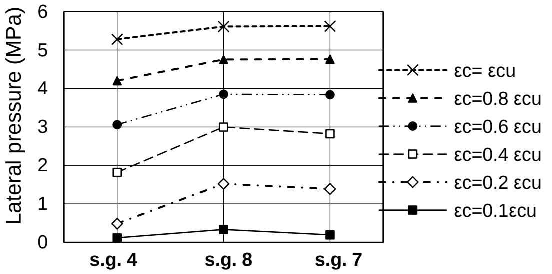


(a) specimen C-12cm-Gst-10cm

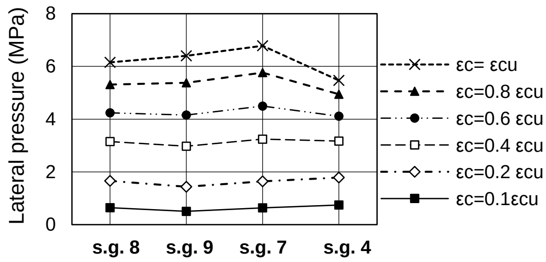


(b) specimen C-12cm-Gst-12cm

Fig. 17 Distributions of lateral confining pressures along the mid-height cross section for different axial strain values

By assuming that the lateral force along the FRP jacket perimeter is constant, as shown in Fig. 16, Eq. (1) may be applied to estimate the local lateral stresses $f_l'$ from the strain gage hoop strains $\varepsilon_{fi}$ considering the characteristics of all FRP layers at the location of each strain gage.

$$f_l^{'} = \frac{2n_f t_f E_f \varepsilon_{fi}}{D} \tag{1}$$

where $n_f$ = number of FRP plies, $t_f$ = FRP jacket thickness, $E_f$ = modulus of elasticity, $\varepsilon_{fi}$ = hoop strain, and D= diameter of cross section.

Figs. 17(a)-(b) show the lateral confining stress distributions for specimens C-12cm-Gst-10cm and C-12cm-Gst-12cm which correspond to the hoop strains depicted in Figs. 11(a)-(b). Confining stress distributions are uniform despite the different hoop strains, as previously reported (Lam and Teng 2004, Lim and Ozbakkaloglu 2015). The observed local divergences of lateral stresses from uniformity have been attributed to a variety of causes, e.g. non-uniform cracking of concrete, bending of lap length at the end parts, geometric discontinuities at the tips of the overlap length (Chen et al, 2010 and 2013). The advent of slippage along the lap length prior to failure is another cause for non-uniformity of hoop strains as discussed in section 3.2.1.

For specimens C-12cm-Gst-10cm and C-12cm-Gst-12cm the measured hoop strain ratios at failure, depicted in Figs. 9(b) and 10(b), are compared to the theoretically predicted ones by application of the equation shown in Fig. 16, in the following. As it is demonstrated, the difference between experimental and theoretical strain ratio values is pretty small (less than 8%) with the exception of the ratios s.g.4/9 and s.g.4/7 in specimen C-12cm-Gst-12cm, because of the smaller experimental strain values of s.g. 4 which have been attributed to the occurrence of local slippage.

- Specimen C-12cm-Gst-10cm:

Measured strain ratio: s.g.4/s.g.7 = 0.38
(theoretical = 0.41)

where the location of strain gages in relation to the underlying layers is as follows (Fig. 3(b)):

s.g.4: GFRP+2CFRP, s.g.7: CFRP

- Specimen C-12cm-Gst-12cm:

Measured strain ratio: s.g.4/s.g.9 = 0.33
(theoretical = 0.41)
Measured strain ratio: s.g.8/s.g.9 = 0.47
(theoretical = 0.50)
Measured strain ratio: s.g.7/s.g.9 = 0.71
(theoretical = 0.69)
Measured strain ratio: s.g.4/s.g.7 = 0.46
(theoretical = 0.59)

where the location of strain gages in relation to the underlying layers is as follows (Fig. 3(c)):

s.g.4: GFRP+2CFRP, s.g.7: GFRP+CFRP, s.g.8: 2CFRP, sg.9: CFRP

### *3.3.2 Square cross-section*

The confinement pressure $f_l'$ applied by FRP continuous sheets in rectangular cross sections may be calculated, among other methods, by multiplying the stresses calculated by Eq. (1) with a reduction factor, $k_s$, that accounts for the reduced effectiveness of confinement compared to a round cross section. In the current study Eq. (2) from Eurocode 8 part 3 (CEN, 2005) is used.

$$f_l^{'} = k_s \frac{2n_f t_f E_f \varepsilon_{ju}}{D} = \frac{2R_c}{D}\frac{2n_f t_f E_f \varepsilon_{ju}}{D} \quad (2)$$

where $k_s = 2R_c/D$, $R_c$ = radius of rounded corners, $n_f$ = number of FRP plies, $t_f$ = FRP jacket thickness, $E_f$ = modulus of elasticity, $\varepsilon_{ju}$ = adopted FRP jacket ultimate strain which is lower than the ultimate strain of FRP, $\varepsilon_{fu}$, and D= larger section width

### 3.3.3 Average lateral stress at cross section

When lateral strains are measured at locations with different FRP layers, an average lateral confining pressure acting at the cross-section, $f_{l,aver}$, may be calculated from Eq. (3). The average lateral confining stresses at failure, $f_{lu,aver}$, calculated for the strains recorded from strain gages at maximum load are included in Table 2. As expected, $f_{lu,aver}$ is lower (about 50%) in GFRP-jacketed specimens compared to similar specimens with CFRP jacket. It is also established that $f_{lu,aver}$ in cubic specimens is about 40% of the respective value in cylindrical specimens for similar jacket characteristics.

$$f_{l,aver} = \frac{\sum f_{li}^{'} \cdot L_i}{L_{tot}} \quad (3)$$

where $f'_{li}$ is the lateral pressure calculated from Eqs. (1) or (2) that acts at a length $L_i$ with the same jacket characteristics along the section's perimeter, $L_{tot}$, for a measured hoop strain, $\varepsilon_{fi}$, (where $\Sigma L_i = L_{tot}$). When multiple strain gages are situated at a length $L_i$ average strains are used.

### 3.4 Estimation of confined concrete strength

The confined concrete characteristics of columns axially loaded in compression are in general calculated taking into account the lateral confining pressure, $f'_l$, exerted by the FRP jacket on the cracked concrete core. Numerous design models for estimating the characteristics of FRP-confined concrete have been proposed, many of which are evaluated against experimental data in previous studies (Lorenzis and Tepfers 2003, Ozabkaloglu and Lim 2013, Nisticò *et al.* 2014). For the cylindrical specimens in this paper Eq. (4) is used (Lam and Teng 2003) because it proved to describe well the behavior of 32 cylinder specimens with identical manufacturing and material characteristics (Moretti and Arvanitopoulos, 2018), while for the cubic specimens Eqs. (5a)-(5b) are applied from Eurocode 2 part 1-1 (CEN 2004).

$$\frac{f_{cc}^{'}}{f_{co}^{'}} = 1 + 3.3\frac{f_{lu,aver}}{f_{co}^{'}} \quad (4)$$

$$\frac{f_{cc}^{'}}{f_{co}^{'}} = 1 + 5.0\frac{f_{lu,aver}}{f_{co}^{'}} \quad \text{for} \quad f_{lu,aver} \leq 0.05 f_{co}^{'} \quad (5a)$$

$$\frac{f_{cc}^{'}}{f_{co}^{'}} = 1.125 + 2.5\frac{f_{lu,aver}}{f_{co}^{'}} \quad \text{for} \quad f_{lu,aver} > 0.05 f_{co}^{'} \quad (5b)$$

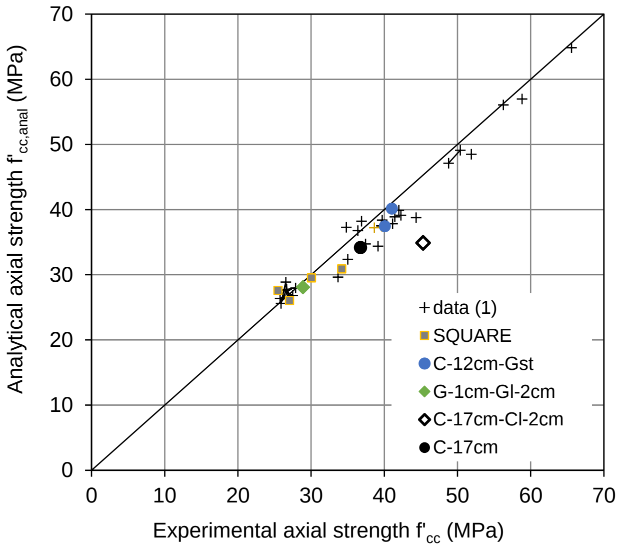


Fig. 18 Comparison between experimental and analytically predicted confined concrete strengths. data (1): available in Moretti and Arvanitopoulos (2018)

where $f'_{co}$ = unconfined concrete strength, $f_{lu,aver}$ = average lateral confining stress at maximum load (included in Table 2)

The comparison between the experimental and the theoretical confined concrete strengths $f'_{cc}$ is good as shown in Fig. 18. Only in case of specimen C-17cm-Cℓ-2cm $f'_{cc,anal}$ is underestimated because Eq. (4) does not account for the contribution of the jacket with longitudinal fibers. The increase in axial strength of specimen C-17cm because of the addition of 1 CFRP jacket with longitudinal fibers may be approximated by the respective increase of axial strength in the similar case for GFRP jackets multiplied by the ratio of the respective axial stiffnesses $(t_f E_f)_{CFRP}/(t_f E_f)_{GFRP}$ = 2.27 according to Eq. (6). (For specimen G-1cm, not included in this study, $f'_{cc}$ = 26.4 MPa, from Moretti and Arvanitopoulos 2018). The issue that the measured confined concrete strength enhancement owing to the jacket with longitudinal fibers relates to the respective axial rigidity of GFRP and CFRP jackets is an indicator of the reliability of test results, despite the fact that only one sample is tested for each configuration.

$$\frac{[f_{cc(C-17cm-C\ell-2cm)}^{'} - f_{cc(C-17cm)}^{'}]}{f_{cc(C-17cm)}^{'}} \approx \frac{(t_f E_f)_{CFRP}}{(t_f E_f)_{GFRP}} \frac{[f_{cc(G-1cm-G\ell-2cm)}^{'} - f_{cc(G-1cm)}^{'}]}{f_{cc(G-1cm)}^{'}} \quad (6)$$

### 3.5 Effectiveness of the FRP jacket schemes tested

The effectiveness of the confining schemes presented in this paper is assessed by means of the ratio of maximum hoop strain to the rupture strain of FRP fibers, $\varepsilon_{h,\max} / \varepsilon_{fu}$, and the cost efficiency confinement index, $Eff_{c,conf}$, which is

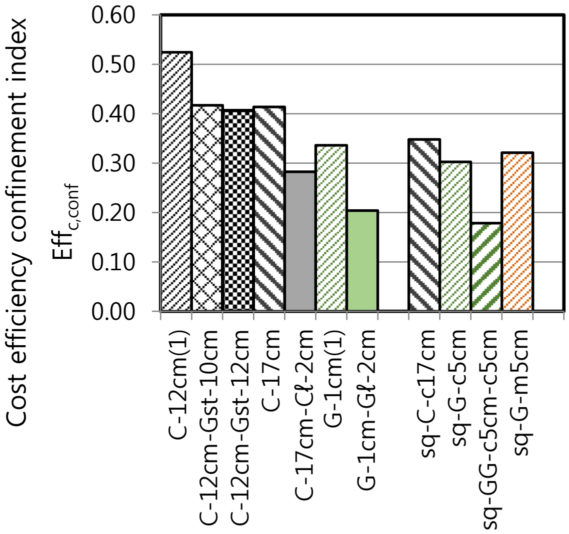


(a) cost efficiency confinement index $\mathrm{Eff}_{c,conf}$

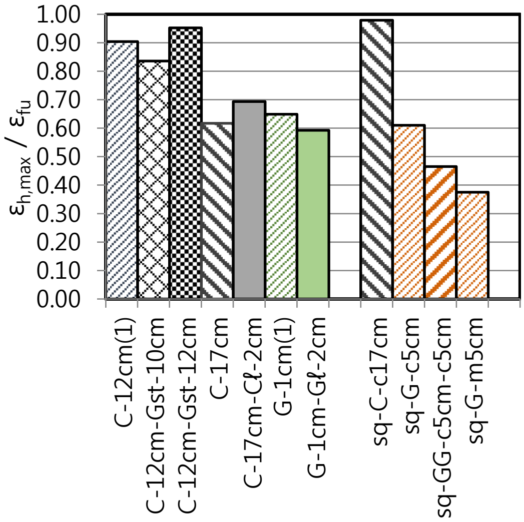


(b) ratio of maximum measured hoop strain to the rupture strain of fibers

Fig. 19 Comparison of the performance of the different FRP schemes tested Data for specimen available in (Moretti and Arvanitopoulos 2018)

calculated from Eq. (7) (Moretti and Arvanitopoulos, 2018), both parameters reported in Table 2. Figs. 19(a)-(b) compare the relative performance of the nine specimens, including that of two companion specimens for the purpose of comparison, i.e. specimens C-12cm and G-1cm. It is noted that comparatively higher $\mathrm{Eff}_{c,conf}$ index is not necessarily linked to higher maximum hoop strains recorded at ultimate load.

$$Eff_{c,conf} = \frac{f'_{cc}}{f'_{co}\,\Sigma(\rho_{fi} k_{ci})1000} \qquad (7)$$

where $\rho_{fi} = t_{fi}\, L_{fi,tot} / A_c$ is the ratio of the cross sectional FRP area of the jacket i-layer (calculated for the nominal thickness, $t_{fi}$, and the total length, $L_{fi,tot}$, including overlap length) to the confined specimen cross section, $A_c$, and $k_{ci}$ is the cost of the respective FRP sheet per meter, normalized by that of CFRP, taken as 77% for GFRP.

From Figs. 19(a)-(b) it is demonstrated that jackets with one layer CFRP are more cost-effective compared to one GFRP layer for both types of cross section, with the increase in the respective performance being more evident in circular compared to square cross sections. Also a trend for lower ratios of $\varepsilon_{h,\max} / \varepsilon_{fu}$ for GFRP compared to CFRP jackets is observed, which is in accordance to the conclusion of Roussakis *et al.* (2007) that for low confinement levels GFRP sheets are strongly affected by material irregularities and stress concentrations. Comparison between cylinders with one CFRP layer shows that specimen C-12cm has the highest $\mathrm{Eff}_{c,conf}$ index between the different anchorage schemes tested, while the addition of a GFRP strip along the end of the FRP lap length resulted in increased ratios of $\varepsilon_{h,\max} / \varepsilon_{fu}$, especially in case of specimen C-12cm-Gst-12cm in which the occurrence of debonding was prevented. Fig. 19(a) also illustrates that the influence of an additional layer with fibers parallel to the axis is not cost effective, in spite of resulting in increased $f'_{cc}$, especially in CFRP jackets. Finally it may be observed that for the square section the presence of two, instead of one, GFRP jackets resulted in an increase of only 60% of $\mathrm{Eff}_{c,conf}$, which conforms to previous findings that multiple FRP layers are less effective (Xiao and Wu 2000, Jiang and Teng 2007, Ilki *et al.* 2008).

## 4. Conclusions

This paper reports the results of an experimental program aimed at improving our understanding on the relative performance of different FRP jacket schemes used for the confinement of concrete columns. Within the limitations of the experimental program, the following tentative conclusions have been drawn.

- One layer FRP jackets proved to be the most cost effective layout compared to the more complicated jacket schemes tested that consist of the same type of material. CFRP jackets were more effective compared to GFRP, both in terms of cost-efficiency and ratio of maximum hoop strain to the rupture strain of FRP fibers, with the increase in the respective performance being more evident in circular compared to square cross sections.
- The location of the lap length in the square cross section did not appear to influence the performance of the specimens for the range of confinement levels investigated. Based on the observations, however, the tips of the FRP lap length should not be close to the location where the side of the section transitions into the quarter-circular corner in order to avoid additive stress concentrations which may lead to FRP rupture.
- For the same jacket characteristics similar maximum hoop strains were measured for circular and square cross sections. Based on the results, maximum hoop strains recorded in the FRP jacket do not seem to be directly

related to the confinement efficiency of the jacket.

- The presence of an external CFRP jacket with fibers parallel to the member's axis is demonstrated to improve the confined concrete strength at a percentage analogous to the axial rigidity of the FRP jacket. Future testing should address the possibility of applying this type of jacket for partial confinement of columns in which there is no possibility of wrapping the whole cross section because of access limitations, especially in columns with low compressive concrete strength and/or inadequate transverse reinforcement for which strength enhancement because of the FRP jacket is expected to be higher.
- Local slippage at the lap length has been observed to result in non-uniformity in the distribution of hoop strains before attaining ultimate load.
- Addition of a GFRP strip at the end of the lap length curtails the occurrence of debonding at the lap length of the underlying jacket owing to the increased capacity of GFRP to deform and hence to redistribute strain localizations without rupture. Future research should address the possibility of adding GFRP strips to reinforce the corners in rectangular FRP wrapped specimens, aiming that the GFRP strips will transfer the jacket stresses away from the geometric discontinuous corners, and thus postpone the FRP jacket rupture.

## Acknowledgments

The author would like to thank Mr. E. Arvanitopoulos who has undertaken the tests reported in this paper as part of his undergraduate thesis, Mr. A. Koutselinis for manufacturing the specimens, Mr. T. Papatheocharis for technical advice at testing, as well as Sika Hellas SA for supplying the composite materials.

## References

Abdelrahman, K. and El-Hacha, R. (2014), "Cost and ductility effectiveness of concrete columns strengthened with CFRP and SFRP sheets", *Polymers,* **6**, 1381-1402. https://doi.org/10.3390/polym6051381.

Au, C. and Buyukozturk, O. (2005), "Effect of fiber orientation and ply mix on fiber reinforced polymer-confined concrete", *ASCE J. Compos. Constr.,* **9**(5), 397-407. https://doi.org/10.1061/(ASCE)1090-0268(2005)9:5(397).

Bisby, L.A. and Take W.A. (2009), "Strain localisations in FRP-confined concrete: new insights", *Proc. ICE*, *Struct. Build.,* **162**(SB5), 301-309. https://doi.org/10.1680/stbu.2009.162.5.301.

Bouchelaghem, H., Bezazi, A. and Scarpa, F. (2011), "Strength of concrete columns externally wrapped with composites under compressive static loading", *Reinf. Plast. Compos.,* **30**(19), 1671-1688. https://doi.org/10.1177/0731684411424333.

CEN (2004), "European Standard EN1992-1-1:2004 Eurocode 2: Design of concrete structures - Part 1-1: General rules and rules for buildings", European Committee for Standardization, Brussels.

CEN (2005), "European Standard EN1998-3:2005 Eurocode 8: Design of structures for earthquake resistance - Part 3: Assessment and retrofitting of buildings", European Committee for Standardization, Brussels.

Chen, G.F., Ai, J. and Stratford, T.J. (2010), "Effect of geometric discontinuities in FRP-wrapped columns", *ASCE J. Compos. Constr.,* **14**(2), 136-145. https://doi.org/10.1061/(ASCE)CC.1943-5614.0000053.

Chen, G.F., Li, J. and Bisby, M. (2013), "Factors affecting the ultimate condition of FRP-wrapped concrete columns", *ASCE J. Compos. Constr.,* **17**(1), 67-78. https://doi.org/10.1061/(ASCE)CC.1943-5614.0000314.

Duran, B., Tunaboyu, O., Kaplan, O. and Avsar, O. (2018), "Effectiveness of seismic repairing stages with CFRPs on the seismic performance of damaged RC frames", *Struct. Eng. Mech.*, **67**(3), 233-244. https://doi.org/10.12989/sem.2018.67.3.233.

Federation international du beton, *fib* (2001), "Externally bonded FRP reinforcement for RC structures", *fib* Bulletin 14. Lausanne.

Fitzwilliam, J. and Bisby, P.E. (2010), "Slenderness effects on circular CFRP confined reinforced concrete columns", *ASCE J. Compos. Constr.,* **14**(3), 280-288. https://doi.org/10.1061/(ASCE)CC.1943-5614.0000073.

Harries, K.A. and Kharel, G. (2002), "Behavior and modeling of concrete subjected to variable confining pressure", *ACI Mater. J.,* **99**(2), 180-189.

Harries, K.A. and Carey, S.A. (2003), "Shape and gap effects on the behavior of variably confined concrete", *Cem. Concr. Research,* **33**, 881-890. https://doi.org/10.1016/S0008-8846(02)01085-2.

Hou, D., Wu, Z., Zheng, J., Zheng, J. and Cui, Y. (2015), "Seismic rehabilitation of substandard RC columns with partially deteriorated concrete using CFRP composites", *Comput. Concr.,* **15**(1), 1-20. https://doi.org/10.12989/cac.2015.15.1.001.

Ilki, A. and Kumbasar, N. (2002), "Behavior of damaged and undamaged concrete strengthened by carbon fiber composite sheets", *Struct. Eng. Mech.*, **13**(1), 75-90. https://doi.org/10.12989/sem.2002.13.1.075.

Ilki, A., Kumbasar, N. and Koc, V. (2004), "Low strength concrete members externally confined with FRP sheets", *Struct. Eng. Mech.*, **18**(2), 167-194. https://doi.org/10.12989/sem.2004.18.2.167.

Ilki, A., Peker, O., Karamuk, E., Demir, C. and Kumbasar, N. (2008), "FRP retrofit of low and medium strength circular and rectangular reinforced concrete columns", *ASCE J. Mater. Civ. Eng.,* **20**(2), 169-188. https://doi.org/10.1061/(ASCE)0899-1561(2008)20:2(169).

Issa, M.A., Alrousan, R.Z. and Issa, M.A. (2009), "Experimental and Parametric Study of Circular Short Columns Confined with CFRP Composites", *ASCE J. Compos. Constr.,* **13**(2), 135-147. https://doi.org/10.1061/(ASCE)1090-0268(2009)13:2(135).

Jiang, T. and Teng, J.G. (2007), "Analysis-oriented stress-strain models for FRP-confined concrete", *Eng. Struct,* **29**, 2968-2986. https://doi.org/10.1016/j.engstruct.2007.01.010.

Kakaletsis, D.J. (2016), "Comparative experimental assessment of seismic rehabilitation with CFRP strips and sheets on RC frames", *Earthq. and Struct.,* **10**(3), 613-628. https://doi.org/10.12989/eas.2016.10.3.613.

Kocak, A. (2015), "Earthquake performance of FRP retrofitting of short columns around band-type windows", *Struct. Eng. Mech.,* **53**(1), 1-16. http://dx.doi.org/10.12989/sem.2015.53.1.001.

Lam, L. and Teng, J.G. (2003), "Design-oriented stress-strain model for FRP-confined concrete", *Constr. Build. Mater.,* **17**(6-7), 471-489. https://doi.org/10.1016/S0950-0618(03)00045-X.

Lam, L. and Teng, J.G. (2004), "Ultimate condition of fiber reinforced polymer-confined concrete", *ASCE J. Compos. Constr.,* **8**(6), 539-548. https://doi.org/10.1061/(ASCE)1090-0268(2004)8:6(539).

Lignola, G.P., Prota, A., Manfredi, G. and Cosenza, E. (2008), "Effective strain in FRP jackets on circular RC columns", *Proceedings of the 4th International Conference on FRP Composites in Civil Engineering*, Zurich, July.

Lim, J.C. and Ozbakkaloglu, T. (2015), "Hoop strains in FRP-confined concrete columns: experimental observations", *Mater.*

*Struct.,* **48**, 2839-2854. https://doi.org/10.1617/s11527-014-0358-8.
Lorenzis, L. and Tepfers, R. (2003), "Comparative study of models on confinement of concrete cylinders with fiber-reinforced polymer composites", *Comp. Constr.* **7**(3), 219-237. https://doi.org/10.1061/(ASCE)1090-0268(2003)7:3(219).
Moretti, M.L. and Arvanitopoulos, E. (2018), "Overlap length for confinement of carbon and glass FRP-jacketed concrete columns", *Comp. Constr.* **195**, 14-25. https://doi.org/10.1016/j.compstruct.2018.04.038.
Moshiri, N., Hosseini, A and Mostofinejad, D. (2015). "Strengthening of RC columns by longitudinal CFRP sheets: effect of strengthening technique", *Constr. Build. Mat.,* **79**, 318-325. https://doi.org/10.1016/j.conbuildmat.2015.01.040.
Nisticò, N., Pallini, F., Rousakis, T., Wu, Y.F. and Karabinis, A. (2014), "Peak strength and ultimate strain prediction for FRP confined square and circular concrete sections", *Compos. Part B,* **55**, 607-634. https://doi.org/10.1016/j.compositesb.2014.07.026.
Ozbakkaloglu, T. and Oelers, D.J. (2008), "Manufacture and testing of a novel FRP tube confinement system", *Eng. Struct,* **30**, 2448-2459. https://doi.org/10.1016/j.engstruct.2008.01.014.
Ozbakkaloglu, T. (2013), "Axial compressive behavior of square and rectangular high-strength concrete-filled FRP tubes", *ASCE J. Compos. Constr.,* **17**(1), 151-161. https://doi.org/10.1061/(ASCE)CC.1943-5614.0000321.
Ozbakkaloglu, T. and Lim, J.C. (2013), "Axial compressive behavior of FRP-confined concrete: Experimental test database and a new design-oriented model", *Compos. Part B,* **55**, 607-634. https://doi.org/10.1016/j.compositesb.2013.07.025.
Pessiki, S., Harries, K.A., Kestner J.T., Sause, R. and Ricles J.M. (2001), "Axial behavior of reinforced concrete columns confined with FRP jackets", *ASCE J. Compos. Constr.,* **5**(4), 237-245. https://doi.org/10.1061/(ASCE)1090-0268(2001)5:4(237).
Raval, R. and Dave, U. (2013), "Behavior of GFRP wrapped RC columns of different shapes", *Proced. Engin.,* **51**, 240-249. https://doi.org/10.1016/j.proeng.2013.01.033.
Rousakis, T.C., Karabinis, A.I. and Kiousis P.D. (2007), "FRP-confined concrete members: axial compression experiments and plasticity modelling", *Eng. Struct.,* **29**, 1343-1353. https://doi.org/10.1016/j.engstruct.2006.08.006.
Rousakis, T.C. and Karabinis, A.I. (2008), "Substandard reinforced concrete members subjected to compression: FRP confining effects", *Mater. Struct.,* **41**, 1595-1611. https://doi.org/10.1617/s11527-008-9351-4.
Sadeghian, P., Rahai, A. and Ehsani, M.R. (2010), "Effect of fiber orientation on compressive behavior of CFRP-confined concrete columns", *Reinf. Plast. Compos.,* **29**(9), 1335-1346. https://doi.org/10.1177/0731684409102985.
Shahawy, M., Mirmiran, A. and Beitelman, T. (2000), "Tests and modelling of carbon-wrapped concrete columns", *Compo Part B-Eng.,* **31**(6-7), 471-480. https://doi.org/10.1016/S1359-8368(00)00021-4.
Smith, S.T., Kim, S.J and Zhang, H. (2010), "Behavior and effectiveness of FRP wrap in the confinement of large concrete cylinders", *ASCE J. Compos. Constr.,* **14**(5), 573-582. https://doi.org/10.1061/(ASCE)CC.1943-5614.0000119.
Smyrou, E. (2015), "FRP versus traditional strengthening on a typical mid-rise Turkish RC building", *Earthq. and Struct.,* **9**(5), 1069-1089. http://dx.doi.org/10.12989/eas.2015.9.5.1069.
Tan, K.H. (2002), "Strength enhancement of rectangular reinforced concrete columns using fiber-reinforced polymer", *ASCE J. Compos. Constr.,* **6**(3), 175-183. https://doi.org/10.1061/(ASCE)1090-0268(2002)6:3(175).
Tunaboyu, O. and Avşar, Ö. (2017), "Seismic repair of captive-column damage with CFRPs in substandard RC frames", *Struct. Eng. Mech.,* **61**(1), 1-13. https://doi.org/10.12989/sem.2017.61.1.001.
Wang, Z., Wang, D., Smith, S.T. and Lu D. (2012), "CFRP-confined square RC columns. I: experimental investigation", *ASCE J. Compos. Constr.,* **16**(2), 150-160. https://doi.org/10.1061/(ASCE)CC.1943-5614.0000245.
Wu, J-F. and Jiang J-F. (2013), "Effective strain of FRP for confined circular concrete columns", *Compos. Struct.,* **95**, 479-491. https://doi.org/10.1016/j.compstruct.2012.08.021.
Youssef, M.N., Feng, M.Q. and Mosalam, A.S. (2007), "Stress-strain model for concrete confined by FRP composites", *Compos. Part B,* **38**, 614-628. https://doi.org/10.1016/j.compositesb.2006.07.020.
Yurdakul, Ö. and Avşar, Ö. (2015), "Seismic repair of captive-column damage with CFRPs in substandard RC frames", *Struct. Eng. Mech.,* **48**, 2839-2854. https://doi.org/10.12989/sem.2017.61.1.001.
Xiao, Y. and Wu, H. (2000), "Compressive behavior of concrete confined by carbon fiber composite jackets", *ASCE J. Mater. Civ. Eng.,* **12**(2), 139-146. https://doi.org/10.1061/(ASCE)0899-1561(2000)12:2(139).

*CC*